Microemulsion and lamellar phases of a vector lattice model

M. W. Matsen* and D. E. Sullivan
Department of Physics and Guelph-Waterloo Program for Graduate Work in Physics, University of Guelph, Guelph, Ontario, Canada N1G 2W1
(Received 14 July 1994)

We examine a three-dimensional vector lattice model for water, oil, and amphiphile mixtures, using the mean-field and Bethe approximations as well as Monte Carlo methods. The Monte Carlo results exhibit three-phase coexistence between water-rich, oil-rich, and microemulsion phases, where the microemulsion has low amphiphile concentration ($\approx$15%) in agreement with experiment. Also present is a floating incommensurate lamellar phase which coexists with the microemulsion at slightly higher amphiphile concentration, similar to lamellar phases observed experimentally. These features are absent in the two mean-field-like approximations and we conclude that, in general, these types of approximations are inappropriate for describing mixtures containing efficient amphiphiles.

PACS number(s): 61.20.Gy, 05.50.+q, 64.60.Cn

I. INTRODUCTION

Under standard conditions, oil and water are highly immiscible, but with the addition of small amounts of amphiphile it becomes favorable for them to mix. Although mixed on a macroscopic scale, water and oil remain separated on a microscopic scale by monolayers of amphiphile. These monolayers may form structures with long-range order as in the lamellar, hexagonal, and cubic phases, or instead may result in a disordered microemulsion phase [1]. The ordered phases, generally, exist at lower temperatures and higher amphiphile concentrations than the microemulsion, which can occur with amphiphile concentrations as low as a few percent. This feature of the microemulsion makes it a phase of particular interest.

In reality, the microemulsion is part of a more general disordered (D) phase. At high temperatures, the D phase is an ordinary simple fluid with virtually no internal structure, but at low temperatures it acquires the distinct short-range structure characteristic of a microemulsion, consisting of fluctuating bicontinuous domains of water and oil separated by a vast layer of amphiphile. Although there is no phase transition to separate these behaviors, several criteria have been introduced for this purpose [2]. The disorder line is one such boundary, defined as the locus where the water-water correlation function changes from being monotonically decaying in the ordinary fluid to oscillatory decaying in the microemulsion. Alternatively, the Lifshitz line is the locus at which the water-water structure function develops a peak at nonzero wave vector, signifying a microemulsion.

There have been a number of model studies [3–6] in which the major aim has been to produce three-phase coexistence between water-rich (W), oil-rich (O), and microemulsion (D) phases. Ideally, the microemulsion that these models exhibit should have a low amphiphile concentration in agreement with experiment. The amphiphile molecules that are present should mainly be found along interfaces between microdomains of water and oil. Also, the water-water correlation and structure functions should exhibit the behavior described above. Surprisingly, this has proven to be a considerable challenge.

Early models for ternary mixtures of water, oil, and amphiphile were usually examined by mean-field-like approximations [7–13]. The most common failure encountered in these studies was the inability to explain how small amounts of amphiphile could produce water-oil miscibility. We will show that this is not a failure of the models but rather of the mean-field-like approximations, which are unable to treat phases with short-range structure like that of a microemulsion. This problem is overcome by using Monte Carlo methods.

In early Monte Carlo work, two-dimensional models were studied, as these require less computational effort. A problem with this work was that once the amphiphile efficiency was great enough to produce a lamellar phase the models no longer seemed to exhibit $W+O+D$ three-phase coexistence [7,14]. In some studies [3,15,16], there was evidence of three-phase coexistence, but it was not very compelling and was likely due to finite-size effects and extremely slow Monte Carlo dynamics. Reference [17] discusses why two-dimensional models do not exhibit this coexistence, and links it to the fact that in two dimensions the amphiphilic monolayers are only one dimensional. Three-dimensional models, on the other hand, have been successful in obtaining three-phase coexistence [4–6,8,18].

In this paper, we study a three-dimensional lattice model for mixtures of water, oil, and amphiphile. First, we examine the phase diagrams of the model using the mean-field and Bethe approximations. We find that these approximations produce unreliable results and we discuss

*Present address: Department of Chemical Engineering and Materials Science, University of Minnesota, Minneapolis, MN 55455.

why this is so. We determine the true behavior of the model using Monte Carlo techniques. These reveal that the model exhibits a $W + O + D$ triple line where the D phase is a microemulsion with low amphiphile concentration. The model is also found to exhibit various lamellar phases, some in which the amphiphilic monolayers are pinned to the underlying lattice with a commensurate period and an incommensurate one where the monolayers float freely from the lattice. Our studies of the transitions involving these and other periodic phases produced by the model are still preliminary, further examination being deferred to future work.

II. MODEL

Various models have been proposed to describe water-oil-amphiphile mixtures, most of which are discussed in a recent review by Gompper and Schick [2]. Here we consider a model introduced earlier [2,3,9,10,14,15,19,20], which is particularly well suited for Monte Carlo techniques. It is a vector lattice model, where the molecules are restricted to sites on a lattice and the amphiphiles are represented by unit vectors that point in the direction of their head groups. In the present work, we use the face-centered-cubic (fcc) lattice because its large coordination number renders it the most realistic lattice for representing a liquid. At each site i on the lattice, we define two state variables, σ_i and $\mathbf{s}_i$. The variable σ_i takes on a value of 1, 0, or -1 if site i is occupied by water, amphiphile, or oil, respectively. When $\sigma_i = 0$, $\mathbf{s}_i$ is a unit vector representing the orientation of the amphiphile molecule at site i, and otherwise $\mathbf{s}_i = 0$. In the same spirit that molecules are only permitted to occupy sites of a lattice, $\mathbf{s}_i$ is restricted to a discrete set of orientations such that it points towards one of the 12 nearest neighbors of site i. Although there is no difficulty in allowing a continuous range of orientations [8], Monte Carlo calculations are considerably simplified if only a finite number are retained.

The Hamiltonian we use is a simplified version of one we introduced earlier [9]. Here we only retain the minimal number of terms necessary to produce the behavior of a microemulsion;

$$H = -J_1 \sum_{\langle ij \rangle} \sigma_i \sigma_j - J_2 \sum_{\langle ij \rangle} (\sigma_i \mathbf{s}_j \cdot \mathbf{r}_{ji} + \sigma_j \mathbf{s}_i \cdot \mathbf{r}_{ij}) + \mu_s \sum_i \sigma_i^2 , \quad (1)$$

where $\langle ij \rangle$ denotes summation over all distinct pairs of nearest-neighbor sites i and j. The unit vector $\mathbf{r}_{ij}$ specifies the direction from lattice site i to site j. The parameter $J_1 > 0$ favors water-oil separation and $J_2 > 0$ gives the amphiphile tails their hydrophobic behavior and the heads their hydrophilic behavior. The particular results presented here are for the case $J_2/J_1 = 2$, which we find corresponds to a reasonably efficient amphiphile. In the last term, μ_s is the chemical potential of the amphiphile. The absence of a chemical-potential term coupling to σ_i means that we are dealing with a balanced system of equal water and oil concentrations.

III. MEAN-FIELD AND BETHE APPROXIMATIONS

In this section, we present the phase diagrams for the above model obtained using the mean-field and Bethe approximations. These approximations are described in detail in our earlier work [9]. Our aim is primarily to examine the reliability of these approximations for models of microemulsions by comparison with Monte Carlo results, which will be presented in the following section.

Besides the three uniform phases, the water-rich (W), oil-rich (O), and disordered (D) ones, we consider a series of commensurate lamellar (L_n) phases. The L_n phase consists of alternating water-rich and oil-rich regions each n layers thick, separated by monolayers of amphiphile, such that its period is $2(n + 1)$. The lamellae are normal to the [111] direction. Other more elaborate commensurate lamellar phases like those present in the axial next-nearest-neighbor Ising (ANNNI) model [21], which we discuss later, are not considered in this section. We also do not consider tubular phases, where water and oil form tubes arranged periodically and separated from one another by films of amphiphile. These latter phases occur at high amphiphile densities ($\rho_s \approx 0.75$), a region of the phase diagram with which we are not concerned.

The mean-field and Bethe approximations produce very similar phase diagrams. Figures 1 and 2 show them in the temperature versus chemical-potential plane. Solid lines denote first-order transitions and dashed lines indicate second-order ones. The W and O phases coexist at small μ_s and the D phase is stable at large μ_s. Between these are regions of stability of the various L_n phases. In both figures, the first four regions for $n = 1$ to 4 are labeled. We find that they continue on sequentially up to at

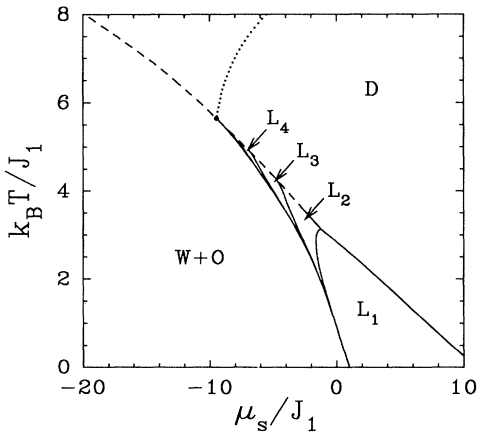

FIG. 1. Mean-field phase diagram plotted in the temperature versus chemical potential plane. Solid lines denote first-order transitions and dashed lines denote second-order ones. The Lifshitz line is indicated with a dotted line and the Lifshitz critical point with a single dot.

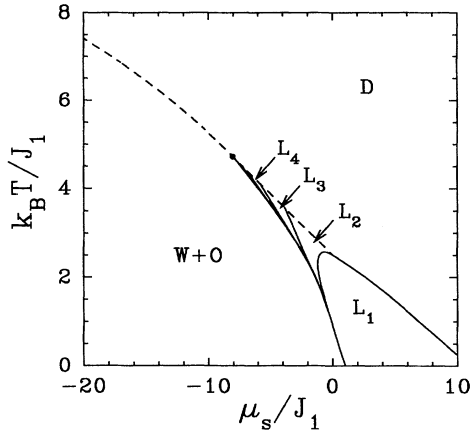

FIG. 2. Same as Fig. 1 except calculated with the Bethe approximation.

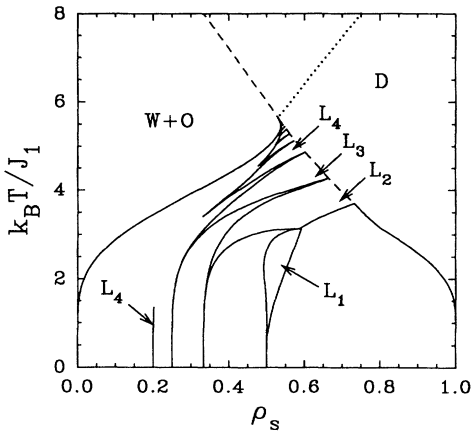

FIG. 3. Mean-field phase diagram plotted in the temperature versus amphiphile density plane.

least $n = 8$ and we suspect up to infinity. These regions of stability for increasing n become smaller and smaller on approaching a Lifshitz critical point [21,22], marked by dots in Figs. 1 and 2, beyond which the $W + O$ region undergoes direct second-order transitions to the D phase.

At low temperatures, the free energy of the phases is reasonably well approximated by $F \approx E_g - TS_g$, where E_g is the ground-state energy and S_g is the ground-state entropy due to the orientational degeneracy of the amphiphile molecules. Comparing these free energies, we find that the $W + O$ and L_1 phases are approximately separated by the line

$$\mu_s = 9J_1 - 4J_2 - k_BT \ln 3 \ . \tag{2}$$

One also finds that if the other L_n phases with $n \geq 2$ exist at low temperatures, they must do so in narrow regions that approximately follow this line. Similarly the transition between the L_1 and D phases is found to occur at approximately

$$\mu_s = 3J_1 + 4J_2 + k_BT(\ln 3 - 2 \ln 12) \ . \tag{3}$$

This transition is only metastable at low temperatures as a tubular phase, noted earlier and not examined here, occurs between the L_1 and D phases.

From an experimental point of view, the grand-canonical phase diagrams in Figs. 1 and 2 are not that meaningful. Furthermore, the experimentally relevant canonical phase diagrams provide important additional information. For these reasons, we also show the phase diagrams in the temperature versus density plane in Figs. 3 and 4. Here, we just label those regions labeled previously and not any of the additional coexistence regions which now appear.

There are only a couple of small topological differences between the mean-field and Bethe phase diagrams. In the Bethe approximation, the entire $D + L_2$ transition is second order whereas in mean field a portion of it is first order. In mean field, we also find that the L_4 phase reappears at low temperatures. It is possible that this happens also in the Bethe approximation at a temperature below $k_BT/J_1 \approx 0.8$. Below this temperature along the line given by Eq. (2), the free energies of the various lamellar phases become too close to determine with certainty their relative stabilities.

For the mean-field phase diagrams, we calculate the Lifshitz line by the method described in Ref. [9]. Because the calculation is much more involved and similar behavior is expected, we do not repeat it for the Bethe approximation. Within mean field, this line, shown with a dotted line in Figs. 1 and 3, is given by

$$\rho_s = \frac{6}{6 + \exp(-\mu_s/k_BT)} = \frac{3}{8}\frac{k_BTJ_1}{J_2^2} \ . \tag{4}$$

This line intercepts the locus of second-order transitions at the Lifshitz critical point. The D phase on the low-temperature side of this line is identified with the microemulsion. We note that in our previous calculations with the current theory [9], using slightly different model interactions on a cubic lattice, a Lifshitz critical point

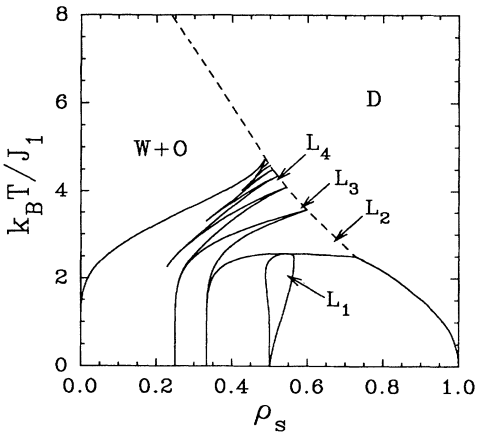

FIG. 4. Same as Fig. 3 except calculated with the Bethe approximation.

did not occur. There, the $W+O$ to D transition line exhibited a tricritical point, becoming first order at lower temperatures, with the Lifshitz line intersecting the locus of first-order transitions. A similar result will occur in the present model for values of $J_2/J_1 < 3/2$.

IV. MONTE CARLO

Figures 5 and 6 show the phase diagrams calculated using Monte Carlo techniques. The Monte Carlo results presented here have been obtained using the heat bath algorithm [23]. With this algorithm, a given site is flipped to a particular state with a probability proportional to the Boltzmann weight, $\exp[-E_i(x)/k_BT]$, where $E_i(x)$ is the energy of site i in state x due to the chemical potential and interactions with its neighbors. Comparing this algorithm to the standard Metropolis algorithm, we find it to be somewhat longer in the time required to perform each Monte Carlo step, but this is more than compensated for by the reduced correlation between Monte Carlo steps. Overall, the heat bath algorithm performs significantly better than the Metropolis one for the model studied here.

The Monte Carlo phase diagrams differ significantly from the mean-field and Bethe results. The first difference is that the $W+O$ to D transition line exhibits both first-order and second-order parts, separated by a tricritical point. To determine the location of the second-order line, we utilize a finite-size scaling method [24] in conjunction with a histogram extrapolation method [25]. Here we use $\mathcal{L} \times \mathcal{L} \times \mathcal{L}$ lattices subject to periodic boundary conditions. For a fcc lattice, each unit cell has four lattice sites and thus the total number of sites, N, is $4\mathcal{L}^3$. Using short runs, we approximately locate the transition at a fixed chemical potential by finding a peak in the heat capacity, $C = (\langle H^2\rangle - \langle H\rangle^2)/k_BT^2$, where angle brackets denote thermodynamic averages. Once this is done, long runs are performed at the approximate temperature for at least three different system sizes, $\mathcal{L}$ [26]. For each $\mathcal{L}$, we calculate as a function of temperature the fourth-order cumulant, $U \equiv 1 - \langle M^4\rangle / 3\langle M^2\rangle^2$, where $M = |\sum_i \sigma_i|$ is the water-oil difference (or magnetization). Its temperature dependence is determined by the histogram extrapolation method as opposed to doing separate runs for different temperatures. In Fig. 7 we show a plot of U versus T for three system sizes from

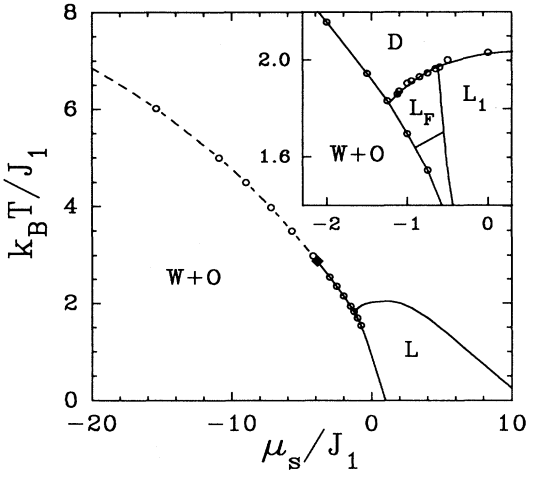

FIG. 5. Monte Carlo phase diagram in the T versus μ_s plane. Circles indicate points calculated by Monte Carlo and the diamond is an estimate of the tricritical point. The inset shows some hypothetical phase boundaries for the lamellar phases. The unlabeled region indicates the approximate region where the long-period commensurate lamellar phases exist.

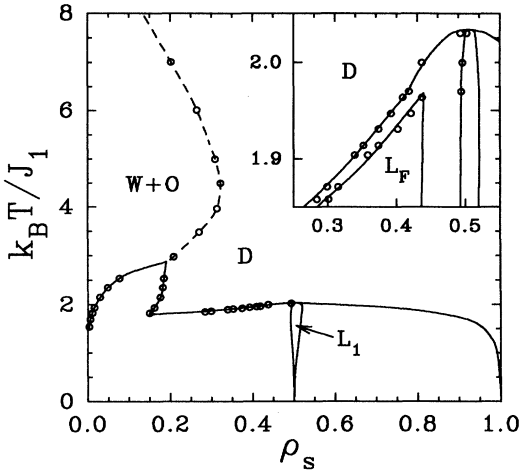

FIG. 6. Monte Carlo phase diagram in the T versus ρ_s plane. Calculated lines are denoted with circles indicating measured points while the other lines are hypothetical. Because the $D + L_F$ coexistence region is so narrow, we only show the region of stability for the L_F phase in the inset.

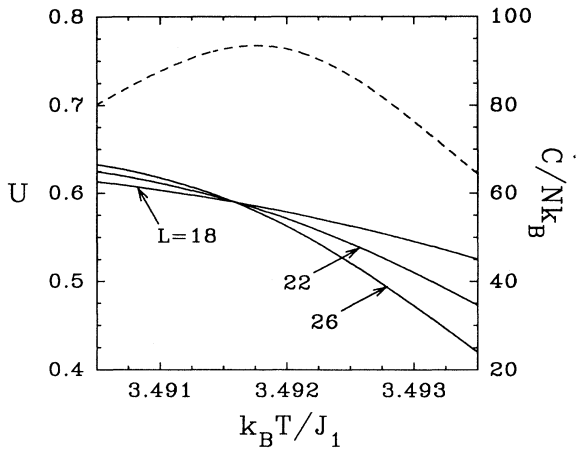

FIG. 7. Plot of the fourth-order cumulant U for three system sizes, $\mathcal{L} = 18$, 22, and 26 (solid lines), and of the heat capacity per lattice site, C/Nk_B, for $\mathcal{L} = 26$ (dashed curve). At this chemical potential, $\mu_s/J_1 = -5.7$, the critical temperature is $k_BT_c/J_1 = 3.4916$.

runs at $k_BT/J_1 = 3.492$ and $\mu_s/J_1 = -5.7$. For each run, the system is allowed to equilibrate for 10^5 Monte Carlo steps (MCS) per site and statistics are collected for the following 10^6 MCS. The curves for $\mathcal{L} = 18$, 22, and 26 cross at the transition, $k_BT_c/J_1 = 3.4916$. If U is plotted as a function of $(T/T_c - 1)\mathcal{L}^{1/\nu}$ using the three-dimensional Ising exponent, $\nu = 0.6294$ [27], the curves approximately collapse onto a single curve. Similarly we find that plotting other quantities, namely, the magnetization, the magnetic susceptibility, and the heat capacity, and scaling these with three-dimensional Ising exponents, causes the data to collapse onto universal curves. From this, we can be confident that the transition we located is second order.

Table I lists the coordinates for some points along the second-order line. The first one, for $\mu_s = -\infty$, corresponds to the spin-$\frac{1}{2}$ Ising model, and is obtained from Ref. [27]. With the exception of the last point at $\mu_s/J_1 = -4.2$, all the points have been determined by the finite-size scaling method described above. For the point at $\mu_s/J_1 = -4.2$, it would be necessary to use exceptionally large system sizes for that method to work. Instead, we have located its position by finding a peak in the heat capacity. Based on our results for $\mu_s/J_1 = -5.7$ (see Fig. 7), we expect this criterion to be reasonably accurate in locating the transition temperature, but with this method one cannot be certain that it is on the second-order line as opposed to the $W + O + D$ first-order line. In fact, based on our results below for the $W + O + D$ triple line, we believe that this point is in close proximity to the tricritical point. We estimate the latter point to occur at $\mu_s/J_1 = -3.9$, $k_BT/J_1 = 2.9$, and $\rho_s = 0.19$.

To calculate the $W+O+D$ triple line, we first locate a hysteresis at a fixed chemical potential and assume that the transition temperature is in the middle of the hysteresis range. If the hysteresis is small, this provides a reasonably accurate estimate of the transition. Then we do two runs at the estimated temperature, one for the W or O phase and another for the D phase, to obtain their amphiphile densities. Our results are shown in Table II. Ideally, large system sizes (i.e., $\mathcal{L} = 26$) should be used in order to avoid finite-size effects. This is possible at the higher temperatures, but at the lower temperatures we have to use smaller system sizes (i.e., $\mathcal{L} = 12$) so that the hysteresis range does not become too large. Fortunately, at the lower temperatures where the first-order transition is strong, it is less important to obtain accurate estimates of the transition temperature because the amphiphile densities have a weaker T dependence at fixed μ_s. For the two runs used to obtain the amphiphile densities, nothing prevents us from using large system sizes.

TABLE I. Monte Carlo results for the second-order $W+O$ to D transition line.

μ_s/J_1	k_BT/J_1	ρ_s
$-\infty$	9.80	0.0
−28.4	8.007	0.133
−21.0	7.010	0.202
−15.4	6.010	0.265
−10.9	4.995	0.309
−9.0	4.495	0.322
−7.2	3.970	0.314
−5.7	3.4916	0.271
−4.2	2.9805	0.208

TABLE II. Monte Carlo results for the $W + O + D$ triple line.

μ_s/J_1	k_BT/J_1	ρ_s $(W+O)$	ρ_s (D)
−3.0	2.5453	0.077	0.185
−2.5	2.3555	0.049	0.182
−2.0	2.1565	0.030	0.176
−1.5	1.945	0.016	0.161
−1.25	1.83	0.011	0.150

For $\mu_s/J_1 = -3.0$, we did not find a hysteresis even for large system sizes such as $\mathcal{L} = 26$. In Fig. 8 we show a histogram for a run of 2×10^6 MCS on an $\mathcal{L} = 26$ lattice at $k_BT/J_1 = 2.5453$. At this point, the first-order transition is weak enough that the system can cross back and forth between the $W + O$ phases and the D phase, producing peaks in the histogram at $\rho_s = 0.077$ and 0.185, respectively. The average time that the system remains in one phase is 3×10^5 MCS. Figure 9 shows slices through equilibrium configurations of the system when it is in the W and D phases. It is interesting to note that the W phase exhibits micelles [see Fig. 9(a)] and that the D phase possesses a well-defined microemulsion structure [see Fig. 9(b)].

Due to slow Monte Carlo dynamics of the lamellar phase as well as a strong temperature variation of the amphiphile densities along the lamellar-disordered transition curve, a different strategy has been employed to locate the latter transitions, based on creating an interface [28]. A lattice consisting of $\mathcal{L}_z$ (111) layers each with $4\mathcal{L}^2$ sites is used, usually with $\mathcal{L}_z$ between two and three times $\mathcal{L}$. Initially, half the lattice is placed in a disordered configuration and the other half in a lamellar state with lamellae parallel to the interface. The sites in the

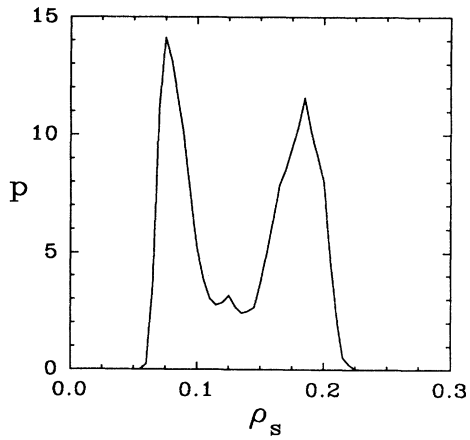

FIG. 8. Histogram showing the normalized probability density p with respect to ρ_s obtained from a run of 2×10^6 MCS on an $\mathcal{L} = 26$ lattice at $\mu_s/J_1 = -3.0$ and $k_BT/J_1 = 2.5453$.

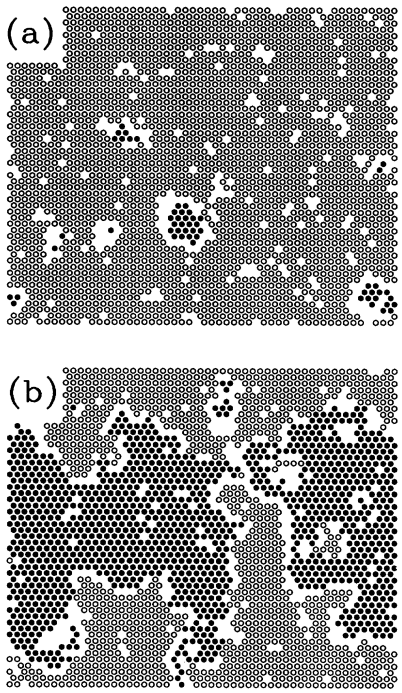

FIG. 9. (111) slices through equilibrated configurations of an $\mathcal{L} = 26$ lattice at $\mu_s/J_1 = -3.0$ and $k_BT/J_1 = 2.5453$. The top one (a) corresponds to the W phase and the bottom (b) to the D phase. For clarity, we only indicate those sites occupied by water (open circles) or oil (filled circles).

uppermost and lowermost (111) layers are kept fixed in their original states, while periodic boundary conditions are used in the other two directions. Usually one phase grows at the expense of the other during the subsequent Monte Carlo run. The transition temperature at fixed chemical potential is that for which both phases remain about equally stable during a run of at least 10^5 MCS. As in the case of the $W + O + D$ triple line, bulk runs using fully periodic boundary conditions are then performed to calculate the thermodynamic properties of the equilibrium coexisting phases. These results are shown in Table III.

The behavior in the neighborhood of the $L + D$ transition indicates that two types of lamellar phase must be distinguished, a commensurate one which we formerly denoted L_1 and a new incommensurate one that we denote L_F. The commensurate L_1 phase is characterized by alternating monolayers of water, amphiphile, and oil molecules, which remain very flat and exhibit few defects [see Fig. 10(a)]. This phase is found at chemical potentials $\mu_s/J_1 \geq -0.6$. We have not explored quantitatively the boundary between this phase and the disordered phase at much larger values of μ_s, but the available data suggest that it approaches the $L_1 + D$ boundaries shown in Figs. 1 and 3. For $\mu_s/J_1 \leq -0.65$, the lamellar phase near the $L + D$ boundary has a much different, thermally roughened character [see Fig. 10(b)] [29]. This exhibits significant fluctuations in the widths of the water and oil regions. Occasionally, passages between adjacent water or oil lamellae also occur. The first-order nature of the transition between this L_F phase and the D phase is supported by the ability to maintain an interface as well as noticeable discontinuities in the amphiphile density ρ_s and mean energy E. Nonetheless, as seen in Table III and the inset of Fig. 6, the jumps in density at the transition are fairly small, less than 6%. The discontinuities in energy are generally larger. These discontinuities, $\Delta\rho_s$ and ΔE, can be related to the slope of the transition line in the T versus μ_s plane through the Clapeyron equation,

$$\frac{dT}{d\mu_s} = -NT\frac{\Delta\rho_s}{\Delta E} \ . \tag{5}$$

We find numerical agreement between both sides of this equation, which lends further support to the first-order

TABLE III. Monte Carlo results for the $L + D$ transition.

μ_s/J_1	k_BT/J_1	ρ_s (D)	ρ_s (L)	Period
−1.125	1.858	0.284	0.301	7.5
−1.10	1.871	0.299	0.315	7.2
−1.00	1.904	0.339	0.358	6.3
−0.95	1.914	0.352	0.374	5.8
−0.85	1.931	0.374	0.402	5.2
−0.75	1.947	0.392	0.421	5.0
−0.65	1.964	0.409	0.437	4.7
−0.60	1.97	0.418	0.494	4.0
−0.50	2.00	0.437	0.496	4.0
0.00	2.03	0.493	0.502	4.0

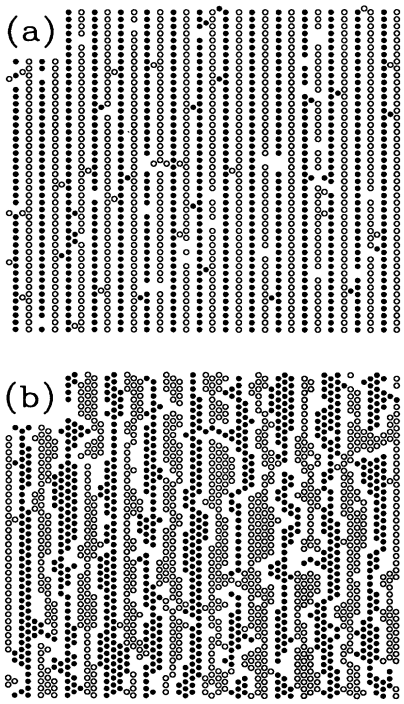

FIG. 10. Equilibrated lamellar configurations on a lattice of size $\mathcal{L}_z = 60, \mathcal{L} = 23$, at (a) $\mu_s/J_1 = -0.50$ and $k_BT/J_1 = 2.0$, and at (b) $\mu_s/J_1 = -1.0$ and $k_BT/J_1 = 1.904$.

nature of the $L + D$ transition. Similarly, we found this equation to be satisfied along the $W + O + D$ triple line.

The major source of uncertainty in our results for the amphiphile density and the period of the L_F phase is due to discretization of their allowed values by the finite system size. This discretization is somewhat alleviated in our interface runs, but persists in our bulk runs which use periodic boundary conditions to determine the equilibrium values of ρ_s and the period. For this reason, these results have generally been averaged over several independent runs using different values of $\mathcal{L}_z$.

As seen by comparing Figs. 1, 2, and 5, the temperature of the $L + D$ boundary for the incommensurate L_F phase is much lower than that of the commensurate L_n phases in the corresponding region of μ_s predicted by the mean-field and Bethe approximations. The fact that fluctuations have driven the transition first order is in agreement with general arguments for roughened phases [2,30] as well as with evidence from studies [31] of the Widom model [32] for microemulsions. It is likely that, below some locus of roughening transitions in the phase diagram, the lamellar phase becomes commensurate. Although we have not attempted to locate such a roughening boundary, evidence for the existence of smooth commensurate lamellar phases at lower temperatures is discussed below. The inset of Fig. 5 indicates the region where they should exist.

The extrapolation of our $L + D$ transition line towards the $W + O + D$ triple line (see Fig. 5) indicates that a $W + O + L + D$ four-phase point exists at $k_BT/J_1 \approx 1.8$. Below this, the $W + O$ phases should transform directly to the lamellar phase. In two dimensions, this should not happen because the microemulsion is thought to extend between the $W + O$ and L regions down to zero temperature [14–16,19], which then prohibits the existence of a $W + O + D$ triple line [17]. Because the triple line is present in three dimensions, there should also be direct transitions between the $W + O$ and L phases, and we do find them. Similarly, we would expect them to occur in the Monte Carlo phase diagram in Ref. [8] if the $W + O$ phase boundary was explored at sufficiently low temperatures.

To determine points along the $W + O + L$ transition, we perform Monte Carlo runs starting from a mixed configuration of W and L phases. At $\mu_s/J_1 = -0.75$, we find that the W phase prevails if $k_BT/J_1 \leq 1.54$ and the L phase dominates for $k_BT/J_1 \geq 1.55$. According to the low-temperature estimate Eq. (2), the transition should be at approximately $k_BT/J_1 = 1.593$. The mean-field and Bethe approximations predict 1.561 and 1.545, respectively. These results all agree quite well. In particular, the Bethe approximation does very well and we expect that it can be trusted as one follows the transition to lower temperatures. For $\mu_s/J_1 = -1.0$, fluctuation effects start to become significant. Here Eq. (2), the mean-field, and the Bethe approximations predict transition temperatures of 1.820, 1.760, and 1.732, respectively. From Monte Carlo, we find the transition to occur between 1.69 and 1.70. The Bethe approximation is still not too bad, but we expect this is about the limit to which it can be trusted. At $\mu/J_1 = -0.75$, we find that the lamellar phase exhibits smooth monolayers of amphiphile locked into the (111) layers of the lattice, but some roughness appears in the lamellae at $\mu_s/J_1 = -1.0$. In both cases, the dynamics are too slow for us to determine the correct amphiphile density and period of the L phase.

Because of the slow dynamics, we used a small system size, $\mathcal{L} = \mathcal{L}_z = 12$, in the Monte Carlo runs for the $W + O + L$ transition. Although this should be sufficient for dealing with W, O, and commensurate L phases where fluctuations are small, it may not be so for the microemulsion phase. In order to be reasonably certain that the microemulsion does not actually penetrate between the $W + O$ and L phases for the cases above, we have also examined a larger lattice. For temperatures in the vicinity of the $W + O + L$ transition at $\mu_s/J_1 = -1.0$ and -0.75, we have started Monte Carlo runs on an $\mathcal{L} = 26$ lattice with an initial configuration obtained from the microemulsion phase at $\mu_s/J_1 = -1.25$ and $k_BT/J_1 = 1.83$. For the runs at $\mu_s/J_1 = -0.75$, we find the curved amphiphilic layers of the microemulsion to be unfavorable, quickly evolving towards flat monolayers which become pinned to the underlying lattice. Thus we are quite certain that the microemulsion as well as the floating incommensurate lamellar phase must be unstable there. For $\mu_s/J_1 = -1.0$, we are quite certain that the microemulsion is unstable but we cannot say the same regarding the L_F phase.

V. DISCUSSION

One of the more striking observations from our results is the inaccuracy of the mean-field and Bethe phase diagrams in comparison to the Monte Carlo ones. Clearly this suggests that one must be cautious when dealing with such approximations. Indications of this have surfaced in previous work [3,4,7,8,14,28]. The explanation for this discrepancy is straightforward, but it is somewhat surprising how large it is and that the Bethe approximation does not improve the situation.

The limitation of mean-field theory is that it cannot deal with short-range order or any type of order that is not pinned to the underlying lattice. Hence it cannot properly treat the microemulsion or the floating incommensurate lamellar phase. It can reasonably well treat the W and O phases as well as the commensurate ordered phases, because in those cases the instantaneous field experienced by a particular lattice site remains nearly constant and can be reliably approximated by its average value, hence validating mean-field theory. For the disordered phase, the instantaneous fields fluctuate significantly and are not at all approximated well by their mean values. At high temperatures, mean-field theory is still adequate, although only because k_BT is large compared to the instantaneous fields and it matters little how poorly the latter are represented. At lower temperatures, where the microemulsion structure sets in, this is no longer true and mean-field theory fails. This also applies to the floating incommensurate lamellar phase.

The inability of mean-field theory to deal with the

microemulsion structure is revealed in numerous ways. For example, in a balanced (i.e., $\langle M \rangle = 0$) microemulsion, the theory predicts that $\left\langle \sum_{\langle ij \rangle} \sigma_i \sigma_j \right\rangle = 0$, indicating that water and oil are homogeneously mixed rather than existing in microdomains separated by amphiphilic sheets as in Fig. 9(b). This also means that the theory evaluates the internal energy E incorrectly. In addition, the theory seriously overestimates the entropy S of a microemulsion. Specifically, in the canonical ensemble (i.e., with concentrations held fixed), it maximizes the entropy, which for the present model gives $S/Nk_B = -\rho_s \ln(\rho_s/12) - (1-\rho_s)\ln[(1-\rho_s)/2]$. For a structureless fluid this is appropriate, but as the Lifshitz line is crossed when T decreases at fixed ρ_s (see Fig. 3), the entropy should decrease, reflecting the development of microemulsion structure within the D phase. In short, mean-field theory incorrectly calculates the free energy, $F = E - TS$, for a microemulsion, which casts doubts on the accuracy of the resulting phase diagram. This problem is inherently related to the absence of correlations within mean-field theory and can only be overcome by using a theory that accounts for correlations.

In many models, such as the spin-$\frac{1}{2}$ Ising model, results obtained by the cluster-variational method converge rapidly to the exact ones with increasing cluster size [33]. Thus the Bethe approximation produces a substantial improvement over mean field, and the Kikuchi approximation offers a similar improvement over that. In the present case, we find the Bethe approximation does not offer a significant improvement over mean field. We expect that very large-sized clusters must be considered for an accurate treatment and thus cluster-variational methods are not appropriate for studying models that produce microemulsions.

Understanding these inadequacies of the mean-field and Bethe approximations allows one to make sense of their phase diagrams. At low temperatures, they produce the correct transition behavior between the W, O, and L_n phases, in this case up to temperatures of about $k_BT/J_1 = 1.7$. At high temperatures, the second-order line is qualitatively correct down to temperatures where the Lifshitz point is predicted. Below this point the two approximations predict weakly structured lamellar phases where the lamellae are pinned to the lattice. If the approximations handled fluctuations correctly, this region would be replaced first by the microemulsion and then by the incommensurate lamellar phase at lower temperatures. This is why mean-field-like approximations have never properly produced microemulsions at low amphiphile concentrations. In the region where the microemulsion should exist, these approximations have instead incorrectly predicted ordered phases.

In some cases, mean-field theories have led to disordered phases with low amphiphile concentrations [8,11], but we point out that these are not due to the physical mechanism embodied in the present model whereby the amphiphile molecules attract water to one end and oil to the other. Instead, these low concentrations result because the amphiphile is treated as a simple impurity which has a favorable interaction with both water and oil. The term $-K_1 \sum_{\langle ij \rangle} \sigma_i^2 \sigma_j^2$ that occurs in the Blume-Emery-Griffiths model can achieve this with $K_1 > 0$. Although such an interaction tends to mix water and oil together, the resulting disordered phase is structureless as opposed to being a microemulsion [11]. The mean-field disordered phase of Ref. [12] also exhibits a low amphiphile concentration along the triple line. In this case, appropriate interactions are used (see end of this section and Ref. [36]), but the calculation still suffers from the problems discussed above and therefore the mean-field phase diagrams in Ref. [12] may be considerably inaccurate. This is supported to some extent by Monte Carlo calculations in Ref. [18].

Although we have not calculated the Lifshitz line using Monte Carlo, we conjecture that its behavior is as follows. At high temperatures, it should behave like the mean-field result but rather than heading towards a Lifshitz point it will likely head towards the point in the second-order line where the amphiphile concentration peaks, $k_BT/J_1 \approx 4.5$ (see Fig. 6). Because the occurrence of a Lifshitz critical point is ruled out by the presence of three-phase $W + O + D$ coexistence in our Monte Carlo results, the Lifshitz line cannot intersect the locus of second-order transitions. Instead, we expect it to follow closely below the line of second-order transitions, eventually intersecting the $W + O + D$ triple line.

Below the microemulsion, we find transitions to ordered lamellar phases. For $\mu_s/J_1 \geq -0.6$, the microemulsion transforms into the commensurate L_1 phase as the temperature is lowered. In this phase, the amphiphilic monolayers are packed tightly together with a period of only four layers, leaving little room for the monolayers to fluctuate. As a result, this phase exhibits flat monolayers that are pinned to the lattice. For lower chemical potentials, a lamellar phase forms with wider layers of water and oil, which allow the amphiphilic monolayers to fluctuate. Such fluctuations free the monolayers from the lattice, resulting in a floating incommensurate lamellar (L_F) phase. In this phase, the period increases continuously with decreasing chemical potential. If the temperature is lowered further, we expect this L_F phase to undergo a transition analogous to a roughening transition and the amphiphilic layers to become flat, locking into the (111) layers of the lattice.

Even with flat amphiphilic layers that lock into the lattice, incommensurate periods would be possible if the widths of the water and oil layers were random. Certainly, random water and oil widths would result in additional entropy that could lower the free energy. However, on evaluating this entropy, one finds that it increases only proportional to $\mathcal{L}$ whereas the volume of the system increases as $\mathcal{L}^3$, and thus it is irrelevant in the thermodynamic limit $N \to \infty$. Thus when lamellae are pinned to the underlying lattice, there is no entropic advantage to forming an incommensurate phase. Instead the widths of the water and oil layers will be determined by fluctuations that mostly involve small-sized clusters, resulting in commensurate lamellar phases such as the L_n phases examined in Sec. III. As well, more elaborate lamellar phases where not all the oil and water layers have equal

widths may occur. We expect behavior similar to that in the ANNNI model, where an infinity of distinct phases, commensurate with the underlying lattice, emerges from a multiphase point at zero temperature [21]. To properly examine these phases would require developing an involved low-temperature series expansion like that considered for the ANNNI model [34].

Reference [8] uses a vector lattice model similar to the present one with only nearest-neighbor interactions, which also produces long-period lamellar phases. However, these phases do not appear in the mean-field results of Ref. [8] as they do here, perhaps due to a small error that occurs in the calculations [35] or perhaps because the authors simply did not consider them. In their Monte Carlo work, they observe both the commensurate L_2 (period-6) and L_3 (period-8) lamellar phases. It is claimed that these phases can evolve into the D phase without passing through a phase transition. As these lamellar phases and the D phase have different symmetries, this should not be possible. We expect that a more careful examination of this region would reveal such transitions and perhaps would also reveal a floating incommensurate phase like the one we observe.

Stockfisch and Wheeler [4] have used Monte Carlo to examine a lattice model which they had earlier introduced and examined by mean-field theory [13]. Their Monte Carlo work primarily focused on demonstrating the existence of three-phase coexistence. They noted that their earlier mean-field results were not reliable and, as well, they found it necessary to introduce additional many-body interactions representing surfactant bending energy effects in order to achieve three-phase coexistence in their Monte Carlo calculations. A similar finding is the necessity to add further many-body interactions to the Widom model of microemulsions [32] in order to produce three-phase coexistence in that model [5]. These features contrast with the present vector model, where the only elements necessary for producing three-phase coexistence are appropriate two-body interactions on a three-dimensional lattice [36]. A further advantage of the present model is that it can account for the more complex topology of the phase diagrams of nonionic amphiphiles [1], on being generalized to include the effects of hydrogen bonding between water and amphiphile [37].

ACKNOWLEDGMENTS

We are grateful to F. Schmid for sharing some of her expertise on Monte Carlo techniques. We also acknowledge M. Zuckermann, K. Elder, M. Schick, and J. A. Forrest for interesting and helpful discussions. D.E.S. wishes to thank M. Zuckermann for his hospitality at the Department of Physics, McGill University, where part of this work was initiated, and likewise, M.W.M. thanks M. Schick for his hospitality at the Department of Physics, University of Washington. This work was supported by the Natural Sciences and Engineering Research Council (NSERC) of Canada.

[1] M. Kahlweit, R. Strey, and P. Firman, J. Phys. Chem. **90**, 671 (1986).
[2] G. Gompper and M. Schick, in *Self-Assembling Amphiphilic Systems*, edited by C. Domb and J. L. Lebowitz (Academic Press, London, 1994).
[3] P. A. Slotte, Phys. Rev. A **46**, 6469 (1992).
[4] T. P. Stockfisch and J. C. Wheeler, J. Chem. Phys. **99**, 6155 (1993).
[5] A. Hansen, M. Schick, and D. Stauffer, Phys. Rev. A **44**, 3686 (1991).
[6] D. Stauffer, N. Jan, Y. He, R. B. Pandey, D. G. Marangoni, and T. Smith-Palmer, J. Chem. Phys. **100**, 6934 (1994).
[7] K. Chen, C. Ebner, C. Jayaprakash, and R. Pandit, Phys. Rev. A **38**, 6240 (1988).
[8] J. R. Gunn and K. A. Dawson, J. Chem. Phys. **96**, 3152 (1992).
[9] M. W. Matsen and D. E. Sullivan, Phys. Rev. A **41**, 2021 (1990).
[10] A. Ciach and J. S. Hoye, J. Chem. Phys. **90**, 1222 (1989); A. Ciach, J. S. Hoye, and G. Stell, *ibid.* **95**, 5300 (1991); A. Ciach, *ibid.* **96**, 1399 (1992).
[11] M. Schick and W.-H. Shih, Phys. Rev. Lett. **59**, 1205 (1987).
[12] G. Gompper and M. Schick, Phys. Rev. B **41**, 9148 (1990); J. Lerczak and M. Schick, Phys. Rev. A **46**, 985 (1992).
[13] T. P. Stockfisch and J. C. Wheeler, J. Phys. Chem. **92**, 3292 (1988).
[14] M. Laradji, H. Guo, M. Grant, and M. Zuckermann, Phys. Rev. A **44**, 8184 (1991).
[15] M. Laradji, H. Guo, and M. Zuckermann, J. Phys. Condens. Matter **6**, 2799 (1994).
[16] G. Gompper and M. Schick, Phys. Rev. A **42**, 2137 (1990).
[17] M. W. Matsen, Phys. Rev. E **48**, 2292 (1993).
[18] F. Schmid and M. Schick, Phys. Rev. E **49**, 494 (1994).
[19] M. W. Matsen and D. E. Sullivan, Phys. Rev. A **46**, 1985 (1992).
[20] A. Ciach, J. S. Hoye, and G. Stell, J. Phys. A **21**, L777 (1988); J. Chem. Phys. **90**, 1214 (1989).
[21] W. Selke, Phys. Rep. **170**, 213 (1988).
[22] R. M. Hornreich, M. Luban, and S. Shtrikman, Phys. Rev. Lett. **35**, 1678 (1975).
[23] A. M. Mariz, F. D. Nobre, and C. Tsallis, Phys. Rev. B **49**, 3576 (1994).
[24] K. Binder and D. W. Heermann, *Monte Carlo Simulation in Statistical Physics: An Introduction*, 2nd corr. ed. (Springer-Verlag, Berlin, 1992), p. 44.
[25] A. M. Ferrenberg and R. H. Swendsen, Phys. Rev. Lett. **61**, 2635 (1988); **63**, 1658 (1989).
[26] At high temperatures, $\mathcal{L} = 10$, 12, and 15 work well, but at lower temperatures, $k_BT/J_1 \approx 4.5$, larger sizes are required, presumably due to the onset of microemulsion structure.
[27] R. J. Creswick, H. A. Farach, and C. P. Poole, Jr., *In-*

troduction to Renormalization Group Methods in Physics (John Wiley & Sons, New York, 1992).
[28] N. Jan and D. Stauffer, J. Phys. (Paris) **49**, 623 (1988).
[29] Independent mean-field Monte Carlo calculations on the present model by F. Leonard and M. Zuckermann (unpublished) have also demonstrated the existence of an L_F phase.
[30] S. A. Brazovskii, Zh. Eksp. Teor. Fiz. **68**, 175 (1975) [Sov. Phys. JETP **41**, 85 (1975)].
[31] K. A. Dawson, B. L. Walker, and A. Berera, Physica A **165**, 320 (1990).
[32] B. Widom, J. Chem. Phys. **84**, 6943 (1986).
[33] D. M. Burley, in *Phase Transitions and Critical Phenomena*, edited by C. Domb and M. S. Green (Academic Press, London, 1972), Vol. 2, p. 329.
[34] M. E. Fisher and W. Selke, Phys. Rev. Lett. **44**, 1502 (1980).
[35] In Ref. [8], the trial Hamiltonian for the mean-field calculations, Eq. (8), should include a term which is quadratic in $\mathbf{s}_n$ in order to be consistent with the underlying model Hamiltonian, if either c_5 or c_6 are nonzero.
[36] A vector model such as that used here can in principle be reduced to one involving many-body spin-dependent interactions by integrating out the orientational degrees of freedom. See Ref. [3] as well as M. S. Skaf and G. Stell, J. Chem. Phys. **97**, 7699 (1992).
[37] M. W. Matsen, M. Schick, and D. E. Sullivan, J. Chem. Phys. **98**, 2341 (1993).